

Development of a Chipscale Integrated Microelectrode/Microelectronic Device for Brain Implantable Neuroengineering Applications

Yoon-Kyu Song, William R. Patterson, *Member, IEEE*, Christopher W. Bull, Joseph Beals, Naejye Hwang, Andrew P. Deangelis, Christopher Lay, J. Lucas McKay, Arto V. Nurmikko, *Fellow, IEEE*, Matthew R. Fellows, John D. Simeral, John P. Donoghue, and Barry W. Connors

Abstract—An ultralow power analog CMOS chip and a silicon based microelectrode array have been fully integrated to a microminiaturized “neuroport” for brain implantable neuroengineering applications. The CMOS integrated circuit (IC) includes preamplifier and multiplexing circuitry, and a hybrid flip-chip bonding technique was developed to fabricate a functional, encapsulated microminiaturized neuroprobe device. Our neuroport has been evaluated using various methods, including pseudospike detection and local excitation measurement, and showed suitable characteristics for recording neural activities. As a proof-of-concept demonstration, we have measured local field potentials from thalamocortical brain slices of rats, suggesting that the new neuroport can form a prime platform for the development of a microminiaturized neural interface to the brain in a single implantable unit. An alternative power delivery scheme using photovoltaic power converter, and an encapsulation strategy for chronic implantation are also discussed.

Index Terms—Brain-computer interface (BCI), integrated neural probe array, low-noise preamplifier, neuroprosthesis.

I. INTRODUCTION

AMONG the several different approaches to intracortical sensors in the form of microelectrode arrays, a silicon-based monolithic unit with up to 100 Pt/PtSi coated electrodes has been particularly successful in sampling the neural activity in the MI region [1]. Chronically implanted, this multielectrode arrangement allows the long term (>1 year) exploration of a significant amount of motor cortex space so that, in conjunction with newly developed decoding techniques using probabilistic analysis [2], good correlation has been achieved for the arm movement of a monkey between the signals recorded directly from the brain (“thought-for-action”) and the real physical action by the animal [3]. First human trials are now under way [4]. However, such multielectrode sensors, whether silicon or

microwire based, presently require cumbersome, complex cabling arrangements and tether the subject to a fixed location.

While a number of efforts are underway to compact the sensing instrumentation associated with the development of a real-time brain-machine interface [5], here, we show first steps of a successful integration and operation of a chipscale unit that integrates a silicon-based multielectrode array with an ultralow power, high-performance silicon micro-electronic integrated circuit. The CMOS integrated circuit contains an array of sixteen low-noise preamplifiers with on-board multiplexing and an output buffer amplifier that enable a significant reduction in the amount of wiring which is required to extract the neural signals from the implanted recording unit for subsequent processing and analysis. The amplifier array is bonded directly to a silicon electrode array and then is wire-bonded to a seven-wire interface and encapsulated with silicone. We believe that our hybrid unit represents a first of its kind and, more importantly, view this accomplishment as a prime platform for the development of a next level of microminiaturized “neuroports” where eventually all required electronics will be part of a single brain-implantable unit. We note that earlier successful effort to integrate amplifiers with a sensor probe by Wise and collaborators [6]. This work is based on silicon blade electrodes with side contacts built using anisotropic etching and with the CMOS circuitry at one end of the assembly. Our geometry offers a number of advantages both for implantation and the critical considerations for ultra-low power operation.

II. CMOS INTEGRATED PREAMPLIFIER ARRAY WITH INTEGRAL MULTIPLEXING

In a CMOS amplifier, one can show that the input-referred thermal noise and power dissipation are inversely related such that the product of noise voltage squared times the power should be constant for a given circuit topology. The best reported value of this quality factor is for a circuit presented by Harrison [7] although it was not designed for the integration of a microelectrode array and had some dc baseline drift. Recently, Mojarradi *et al.* [8] presented a design that, like our system, is aimed at eventual integration to a set of electrodes. More recently, efforts at Duke University have been presented by Obeid, *et al.* [9] for integrated circuits to make very small and efficient hybrid head stage systems by incorporating all amplification and filtering operations for 16 channels into single chips. Because of

Manuscript received December 21, 2004; revised February 18, 2005; accepted February 21, 2005. This work was supported by the BioInfoMicro Program at the U.S. Defense Advanced Research Projects Agency under Grant MDA972-00-1-0026.

Y.-K. Song, W. R. Patterson, C. W. Bull, J. Beals, N. Hwang, A. P. Deangelis, C. Lay, and J. L. McKay are with the Division of Engineering, Brown University, Providence, RI 02912 USA (e-mail: yoon-kyu_song@brown.edu).

A. V. Nurmikko is with the Department of Physics and Division of Engineering, Brown University, Providence, RI 02912 USA.

M. R. Fellows, J. D. Simeral, J. P. Donoghue, and B. W. Connors are with the Department of Neuroscience, Brown University, Providence, RI 02912 USA.

Digital Object Identifier 10.1109/TNSRE.2005.848337

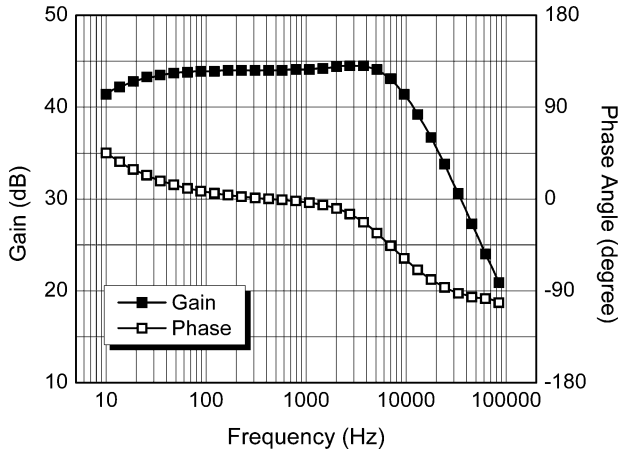


Fig. 1. Bode plot of the response of one channel of the amplifier IC.

high power dissipation, these circuits seem unlikely candidates for implantation.

In the overall architecture of our CMOS amplifier array, the preamplifiers each possess an input bonding pad within its own area of the integrated circuit. We have built our prototypes for a 4×4 microelectrode array (1.6×1.6 mm), but all designs and fabrication are compatible with the presently standard full 10×10 arrays, and beyond. The amplifier array pitch of $400 \mu\text{m}$ exactly matches that of the array of extracellular electrodes so that bonding each input pad to its corresponding electrode can be done by epoxy ball bonding, as outlined in Section III. Each amplifier also has a CMOS transmission gate switch attaching its output to a column line under control of a row select line. Amplifier outputs are routed to the output buffer amplifier by row and column selection implemented with a digital row decoder and an analog column multiplexer also based on CMOS switches. A total of only seven wires is needed as the interface to the chip, including four source select lines, output, power, and ground. The circuit was fabricated on a 2.2×2.2 mm chip in the AMIS $1.5 \mu\text{m}$ process. A detailed design and performance characteristics of the integrated circuit would be found in the previous publication by the authors [10].

Our design choices were most heavily constrained by power considerations, which suggested the need to be as near to $50 \mu\text{W}$ per amplifier as practical so that a scaled-up version would present acceptable thermal loading of the tissue in contact with it (our worst-case thermal model showed about 1°C temperature rise at the center contact point of a 10×10 channel device). Fig. 1 and Table I summarize the principal performance parameters of the final design.

III. PHYSICAL INTEGRATION OF THE MULTIELECTRODE ARRAY WITH CMOS CHIP: A HYBRID NEUROPROBE

We have chosen to use a flip-chip integration strategy based on a carefully chosen conductive epoxy for the electrical interface between the electrode array and the CMOS chip. This approach has two advantages: first it limits the stresses of pressure and temperature on the base of the electrode array and second, it eliminates the stress that soldering or ultrasonic bonding would

TABLE I
PERFORMANCE OF THE AMPLIFIER IC

Parameter	Simulation	Measurement
Noise (RTI)	$6.8 \mu\text{V}_{\text{RMS}}$	$9 \mu\text{V}_{\text{RMS}}$
Power per amplifier	$52 \mu\text{W}$	N/A
Power	1.3 mW	1.4 mW
High frequency cutoff (-3 dB)	7.5 kHz	7.3 kHz
Low frequency cutoff (-3 dB)	5 Hz	10 Hz
Overload recovery (200 mV step)	N/A	745 ms

place on the double polysilicon input capacitor structure of the chip, increasing its reliability. Conductive silver epoxy (Epotek Model H20E-PFC) is applied to the pads ($80 \times 80 \mu\text{m}$) of the CMOS chip by a pin stamping technique so that approximately $150\text{-}\mu\text{m}$ diameter and $50\text{-}\mu\text{m}$ high epoxy dots are deposited with $20 \mu\text{m}$ placement precision. The 16-element microelectrode arrays were bonded to the CMOS chip by using a high-accuracy, manual flip chip and die bonder. Key steps in the process require that the electrode set is first placed on a glass podium, the height of which ultimately fixes the deformation and finished height of the epoxy posts that connect the electrodes to the amplifiers.

We used a placement guide made from GaAs plates to hold and align the microelectrode array. The fixture was transferred to the flip chip bonder where its gold base pads are aligned with the pin-stamped epoxy dots on the amplifier IC chip. The two parts were put together slowly to a final bonding pressure. Finally, the epoxy was thermally cured. For test purposes, we attached the hybrid neuroprobe by conductive epoxy to a 0.25-mm-thick alumina support plate with patterned thin film gold wiring to connect it to the rest of the system electronics and optoelectronics. The detail of the assembly procedure were schematically illustrated in [10]. We emphasize that *the integration approach is fully scalable to large microelectrode arrays (100 recording channels and beyond) and that the choice of a 16-channel system was made for test development purposes only*. Fig. 2 shows a photographic view of the hybrid integrated unit prior to and after the silicone encapsulation.

The integrated encapsulated assembly, supported mechanically by the alumina plate, was subsequently mounted to a thin aluminum rod attached to a micromanipulator that enabled positioning and inserting our neuroprobe in a laboratory test system. The system was designed both to test the hybrid neuroprobe and to exercise a signal extraction, processing, and transmission system which included a low power analog-to-digital converter (40 ksp/s per channel at 12-b) controlled by a complex programmable logic device (CPLD)-based programmable timing circuit. The ADC output drives a fiber-optic transmitter that couples the serial data stream (15.36 Mb/s) to a photoreceiver, the output of which goes into a personal computer (PC) through a National Instruments (Model PCI-6533) high-speed digital IO board for data storage, display and processing. The optical links are suitable eventually for very high speed data transmission without electromagnetic interference ($>10 \text{ Gb/s}$) and offer significant advantages for compatibility with biological systems both through material compatibility and through minimizing sites for infection or inflammation.

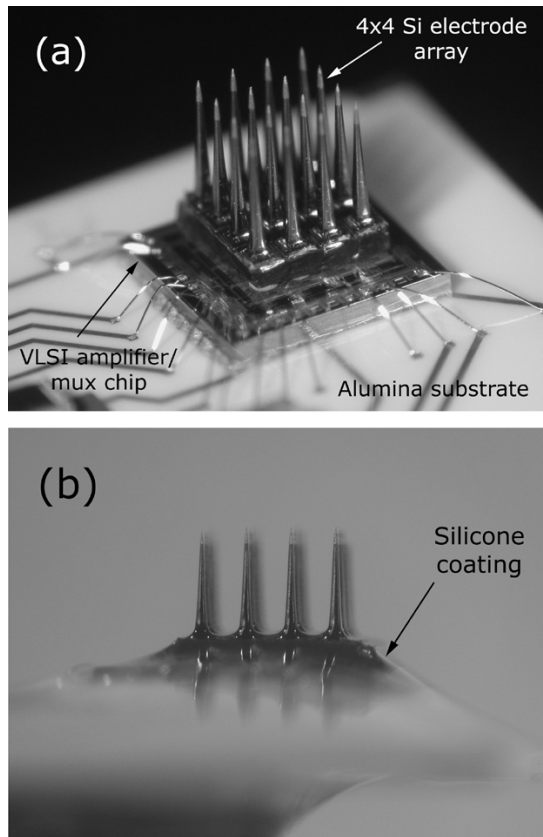


Fig. 2. Electrode and amplifier assembly (a) prior to and (b) after silicone encapsulation.

IV. PERFORMANCE EVALUATION OF THE HYBRID NEUROPROBE

The integrated neuroprobe was evaluated by several methods. First, it was characterized by immersing its probe electrodes into a standard ACSF, a physiological saline solution with resistivity of a few hundred $\Omega \cdot \text{cm}$. An AgCl coated silver electrode was also immersed in the saline bath a few centimeters away from the probe set to act as the reference electrode. By applying a periodic pseudospike signal from an arbitrary function generator (Agilent Model 33 120A) through this reference electrode, we could test all the silicon microelectrode probes simultaneously. Typical spike parameters, 2-ms-long bipolar signal with peak-to-peak amplitudes ranging 100–500 μV , were used to simulate neural signals. An example of these results is shown in Fig. 3, which shows the system output voltage recorded at the PC for three different levels of excitation. This result clearly indicates that our integrated neuroprobe is indeed suitable for recording neural activities such as action potentials. As a cross-comparison, we applied the same test scheme to a Cerebus128 system, a commercial product of Cyberkinetics, Inc., with a 10×10 microelectrode array. The Cerebus128 system showed comparable performance to our fully implantable neuroprobe, with slightly better signal-to-noise ratio.

To further evaluate the functionality of individual channels, we introduced a local excitation method, where the pseudospike signal is localized by a micromanipulator controlled, 100- μm -thick teflon coated Pt-Ir wire excitation electrode. Only about 50 μm at the tip of a wire was exposed to the saline solution, and the exposed part of the wire was placed near ($\sim 20 \mu\text{m}$)

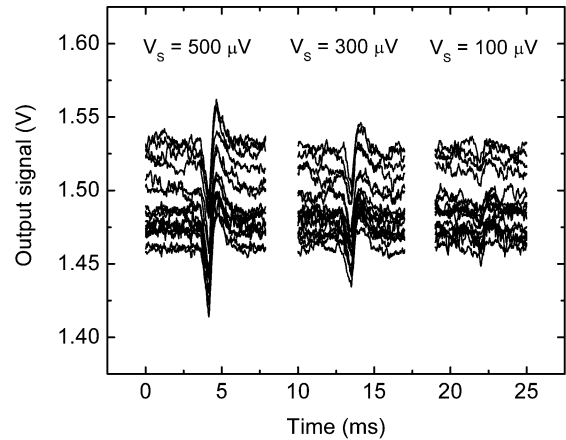


Fig. 3. Amplifier output for the pseudospike excitation in ACSF solution, showing detection capability of the hybrid neuroport. Raw data with various amplitude pseudospike suggests the system detection limit below 100 μV .

one of the electrodes. An AgCl coated silver electrode was used as a ground reference, located at a few centimeters away from the probe. A pseudospike signal is applied between the Pt-Ir excitation electrode and the silver reference electrode, and the potential decay profile is detected by a multielectrode array. Fig. 4 shows (a) a schematic of the experiment, and (b) an example of such a potential profile detected by our 4×4 multichannel hybrid neuroprobe.

Assuming a potential is applied to a small metallic sphere in homogeneous medium with resistivity ρ , a simple electromagnetic model predicts the potential drops inversely proportional to r , distance from the source of excitation. If the medium is saline solution, one should also consider a formation of electric dipole layer at the interface of metal sphere and the electrolyte solution, which forms simply a capacitor. If time-varying potential applied to the sphere with frequency about 1 kHz, one would expect an attenuation and differentiation of the potential, since the resistance of small sphere and a dipole capacitor would act as a high-pass RC filter at the sphere, with cut-off frequency well above the signal frequency in usual saline concentration. In this experiment, we have used diluted (1:10 with DI water) ACSF to alleviate such an issue.

As seen in Fig. 4(b), the result was in a good agreement with the theory, and clearly demonstrates local probing capability of the neuroprobe. In actual brain environment, the neuronal signal would be even more localized than this simple saline case due to inhomogeneity in resistivity of closely packed glial cells with higher conductivity near the electrodes caused by local rupture of the glial cells [11].

In a second set of proof-of-concept experiments, we employed the multielectrode integrated neuroprobe in *in vitro* experiments on thalamocortical brain slices from rats. With the bath application of picrotoxin, we induced spontaneous neural activity in the brain slices, whose telltale signature of local field potential activity is shown in Fig. 5, recorded from one typical electrode. Rhythmic oscillatory field potentials were measured with a signal amplitude approximately 0.5 mV and the period of the neural activity in the range of 80–120 ms, which is consistent with the result recorded by conventional laboratory systems using an ACSF-filled glass pipette electrode. These

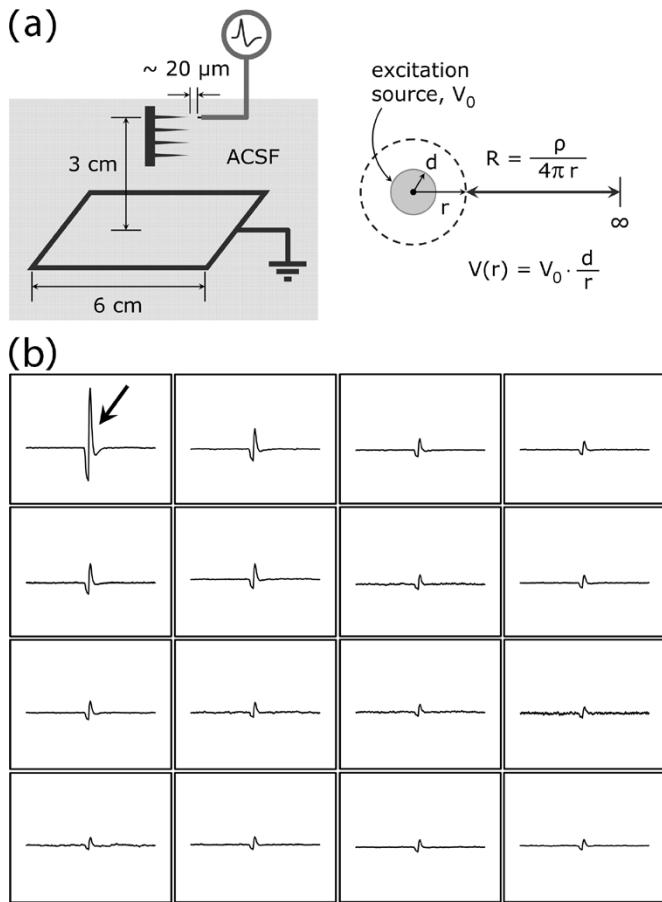


Fig. 4. (a) Schematic of experimental setup (left), and a diagram illustrating a simple electromagnetic theory (right). (b) Potential profile detected by 4×4 multielectrode array in hybrid neuroprobe. An excitation electrode was brought near ($\sim 20 \mu\text{m}$) the tip of an electrode connected to Channel 1 (indicated by an arrow, located upper left corner of 4×4 multielectrode array when viewed from the top). Each graph was averaged over 50 spikes to reduce noise, and the window of each plot corresponds to $0.2 \text{ V} \times 20 \text{ ms}$.

in vitro results thereby suggest that the hybrid neuroprobe assembly with our particular integration strategy offers a performance comparable to that of the present conventional laboratory neural recording systems.

Finally, the hybrid neuroport was acute implanted in primary motor cortex (MI) of *macaca mulatta* monkeys *in vivo* under anesthesia. The results of these experiments are under detailed analysis and will be published elsewhere.

V. INTEGRATION OF OPTOELECTRONICS: PHOTOVOLTAIC ENERGY CONVERTER

The choice of electrical power sources and the delivery of energy to implanted biomedical devices that encapsulate active electronic components is a perennial and major issue. Energizing these devices inductively through the skull is one viable option although it may be difficult, given the power, electromagnetic interference, and heating issues. Here, we consider an alternative concept, namely a microscale photovoltaic energy converter that can be integrated onto an implantable neuroport, for example, and which is supplied optical energy by an optical fiber that can be threaded from the abdominal cavity

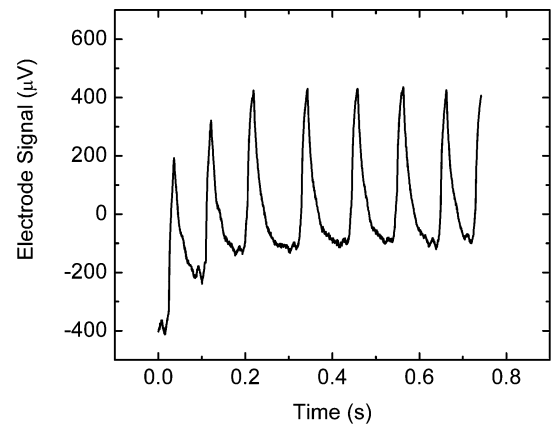


Fig. 5. Typical recording of the oscillatory local field potential response in a thalamocortical brain slice of a rat induced by bath application of picrotoxin.

to the microchip location in the brain. Such a power delivery scheme would be particularly advantageous when a fiber optic cable is already used as broadband neural data transmission link as mentioned in the earlier section.

Our photovoltaic energy converter is based on GaAs/AlGaAs semiconductor p-n-junctions. A $3\text{-}\mu\text{m}$ -thick unintentionally doped GaAs layer sandwiched by $\text{Al}_{0.3}\text{Ga}_{0.7}\text{As}$ p-n junction was grown on semi-insulating GaAs substrate by molecular beam epitaxy (MBE). To facilitate lateral current flow, we used a thin n^+ -GaAs/ $\text{Al}_{0.1}\text{Ga}_{0.9}\text{As}$ (20/150 nm, $n = 2 \cdot 10^{19} \text{ cm}^{-3}/1 \cdot 10^{19} \text{ cm}^{-3}$) and a thick p^+ -GaAs ($0.45 \mu\text{m}$, $p = 5 \cdot 10^{19} \text{ cm}^{-3}$) current spreading layers on n (window) and p (substrate) sides, respectively. As shown in the Fig. 6(a), the device consists of three laterally segmented and serially connected GaAs photocells fabricated by standard microelectronic fabrication process, to generate the requisite total voltage level ($>3 \text{ V}$). The overall optical-to-electrical power conversion efficiency of a completely packaged device was reasonably high about 20%, considering our device has relatively large inactive area for etched segmentation channel without antireflection coating on the window. Also, no particular effort has been made for optimizing coupling of light from multimode fiber to the device. While we expect that significant further improvement (power conversion efficiency well above 50%) is possible, the present device shows a useful proof-of-concept demonstration and is being incorporated into our own microscale integrated neuroport devices as point-to-point sources of energy delivery.

Fig. 6 shows our integrated neuroport powered by a photovoltaic energy converter described above. An 850-nm laser diode and a multimode fiber link were used to provide optical power to the energy converter, which delivers electrical power to the power terminal of our neuroport device. The optically powered neuroport was evaluated with a test scheme described in the Section III, where a sinusoidal input signal was applied in saline solution instead of pseudospikes signal. Although an ultimate system would have no electrical connection between the neuroprobe and support electronics, the metallic wire connection in the serial data link still exists in this demonstration system. As a comparison, the same device was electrically

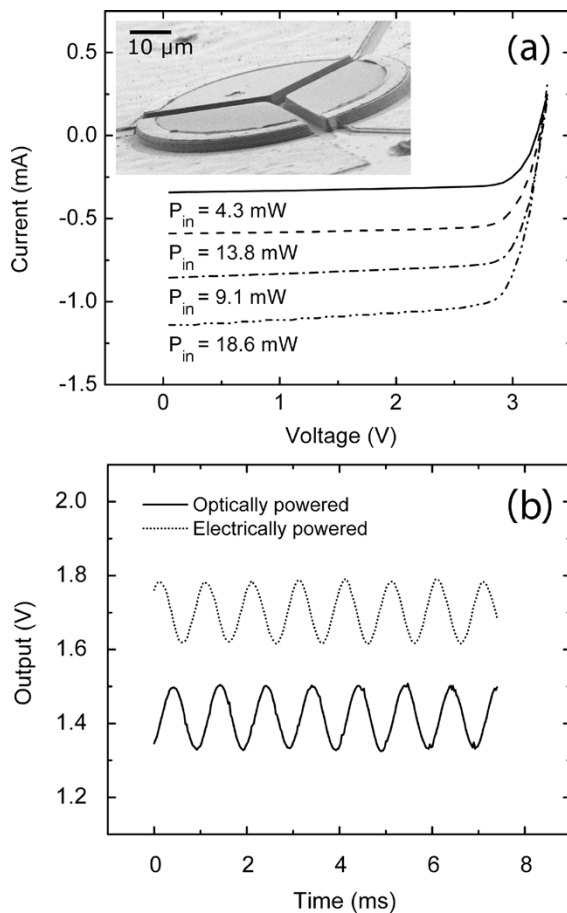


Fig. 6. (a) Typical current-voltage characteristics of the photovoltaic device under various illuminations. Inset: a scanning electron microscope image of a fully fabricated energy converter device with total active diameter of $62.5 \mu\text{m}$. Etched channels separating each segments are clearly visible. (b) An optically powered neuroprobe showing identical characteristics to the one powered by a conventional electrical power supply. The dc levels are shifted for clarity. Optical power required to operate the device (IC chip) was approximately 7 mW .

powered and evaluated with the same test setup, and the characteristics of the neuroports in the two different power delivery schemes were essentially identical, as shown in Fig. 6(b).

VI. ENCAPSULATION AND DEVICE RELIABILITY

Isolating active electronics from exposure to body fluids and the body from potentially harmful materials remains a critical issue in the implementation of chronic neural prosthetics. Neural prosthetics presents unique problems. When designing implants, one likes to exploit the thickness of barrier layers—the thicker the layer, the less likely it is to fail. Unlike other implants, the space into which the device must fit it is limited and the distance between the probe tip and the electronic circuitry is typically less than a few millimeters. These constraints demand a careful choice of materials and strict attention to the processing. The hybrid neuroprobe described earlier is an assembly of active and passive components attached to an alumina substrate. Donaldson [12] and Edell [13] have independently suggested/concluded that silicone elastomers are the most viable encapsulant currently available when convenience, compatibility, and ease of processing are factored into the selection.

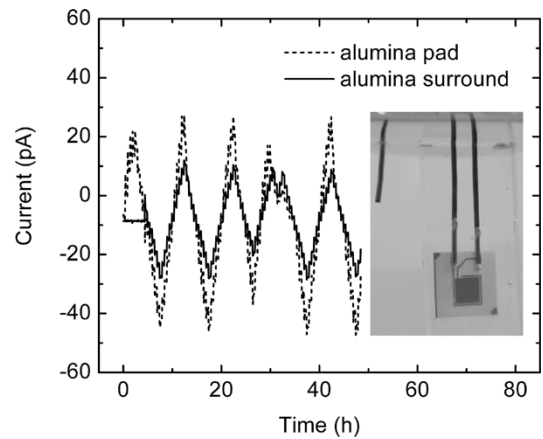


Fig. 7. Representative data from encapsulation current leakage tests (reference electrode driven, guard ring at ground). Inset: an alumina substrate with gold conductors encapsulated in silicone in 0.9% saline solution. The other wire is a platinum reference electrode.

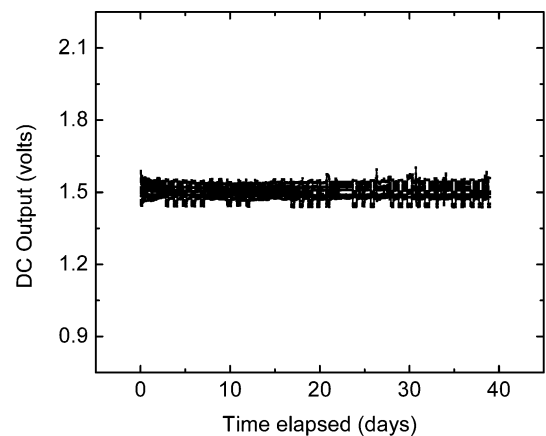


Fig. 8. Typical life test data for a silicone (NuSil 2188) encapsulated assembly. Life tests monitor the output of a device immersed in 0.9% saline solution at room temperature. Steps in the data are due to light sensitivity.

The two short term failure mechanisms are pinholes in the coating and voids at electrically active surfaces. Pinholes allow direct communication of fluid to sensitive electronics producing immediate failure. These can usually be avoided by casting (rather than dipping or brushing) the encapsulant. Silicone passes water vapor which can condense in voids in the material. If there are voids coincident with conductors failure will occur, although not as rapidly as with pinholes. To avoid these problems it is essential that the surfaces are free from contaminants and that the preparation and curing of the elastomer proceed with great care.

In order to evaluate both materials and processes for chronic neural implants, we have developed a test system that allows fairly rapid discrimination of suitable solutions. The connections in the circuit are flexible allowing a variety of paths for current flow. Fig. 7 shows a one type of test sample, an alumina substrate with two gold conductors. This specimen allows measurement of leakage current across the alumina and through the silicone encapsulant. The current test protocol steps a drive voltage from -5 to $+5 V_{DC}$ in 1-V increments. The voltage is held for several readings and a corresponding current time plot is shown in Fig. 4 for a representative recent test in our laboratory.

We have also tested the long term reliability of an actual hybrid neuroprobe under continuous operation, immersed in 0.9% saline solution. We monitored the DC output level, which has a good correlation with the functionality of a device due to high sensitivity of bias stabilization circuitry to any leakage current. Fig. 8 shows a typical life test data for 40 days of operation in saline solution. The stable dc output indicates that the device has not been degraded. In order to verify the stability in dynamic parameters of amplifiers, the device was fully characterized after 70 days of continuous operation in saline solution, and no noticeable change in device parameters was found. We are currently testing devices in saline solution at an elevated temperature (up to 50°C) to accelerate failure mechanisms.

VII. CONCLUSION

In this paper, we have described our recent progress in the development of a functional implantable “neuroport,” where a very low power/low noise CMOS preamplifier and integral multiplexer chip have been integrated to a silicon-based microelectrode neural probe array. We have evaluated the performance of the fully packaged and encapsulated hybrid unit by several testbed methods, and showed its capability of detecting neural activities such as action potentials. *In vitro* experiments using rat brain slices and ongoing *in vivo* testing in (acute) anesthetized monkeys suggest practical prospects of employing the neuroport in practical neural recording applications where portability of equipment is important. Current work aims to add further microelectronic processing power to the chip-scale integrated unit, including low power analog-to-digital conversion.

Our integrated device can be readily scaled to larger microelectrode arrays (100 elements and beyond) without a significant thermal load in a brain tissue environment. In this case, the anticipated high digital signal data rates call for critical evaluation of the choice for telemetry that can supply the necessary broad bandwidth for data transmission, and pose compatibility demands for the stringent physiological constraints within the skull of test animals, and eventually of human subjects. Integration of an optoelectronic data link to the neuroport could be an attractive solution, where a fiber optics is employed both for broadband neural signal transmission and remote power delivery.

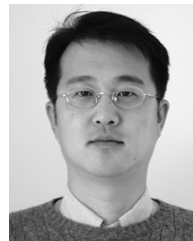
ACKNOWLEDGMENT

The authors would like to thank Dr. I. Ozden and S. Venkataramani for their expertise and participation in the project.

REFERENCES

- [1] K. E. Jones, P. K. Campbell, and R. A. Normann, “A glass/silicon composite intracortical electrode array,” *Ann. Biomed. Eng.*, vol. 20, pp. 423–437, Jul. 1992.
- [2] W. Wu, M. J. Black, D. Mumford, Y. Gao, E. Bienenstock, and J. P. Donoghue, “A switching kalman filter model for the motor cortical coding of hand motion,” in *Proc. IEEE Engineering in Medicine and Biology Soc.*, 2003, pp. 2083–2086.
- [3] M. D. Serruya, N. G. Hatsopoulos, L. Paninski, M. R. Fellows, and J. P. Donoghue, “Instant neural control of a movement signal,” *Nature*, vol. 416, pp. 141–142, Mar. 2002.

- [4] M. D. Serruya, A. H. Caplan, M. Saleh, D. S. Morris, and J. P. Donoghue. The Baingate pilot trial: building and testing a novel direct neural output for patients with severe motor impairment. presented at *Soc. Neuroscience 34th Annu. Meeting*. [Online] http://www.tech-house.brown.edu/~dmorris/publications/SFN2004.ck_poster.pdf
- [5] D. R. Kipke, R. J. Vetter, J. C. Williams, and J. F. Hetke, “Silicon-substrate intracortical microelectrode arrays for long-term recording of neuronal spike activity in cerebral cortex,” *IEEE Trans. Neural Syst. Rehab. Eng.*, vol. 11, no. 2, pp. 151–155, June 2003.
- [6] K. D. Wise, D. J. Anderson, J. F. Hetke, D. R. Kipke, and K. Najafi, “Wireless implantable microsystems: high-density electronic interfaces to the nervous system,” *Proc. IEEE*, vol. 92, no. 1, pp. 76–97, Jan. 2004.
- [7] R. R. Harrison and C. Charles, “A low-power low-noise CMOS amplifier for neural recording applications,” *IEEE J. Solid-State Circuits*, vol. 38, no. 6, pp. 958–964, Jun. 2003.
- [8] M. Mojarradi, D. Binkley, B. Blalock, R. Andersen, N. Ushioefer, T. Johnson, and L. Del Castillo, “A miniaturized neuroprosthesis suitable for implantation into the brain,” *IEEE Trans. Neural Syst. Rehab. Eng.*, vol. 11, no. 1, pp. 38–42, Mar. 2003.
- [9] I. Obeid, J. C. Morizio, K. A. Moxon, M. A. L. Nicoletis, and P. D. Wolf, “Two multichannel integrated circuits for neural recording and signal processing,” *IEEE Trans. Biomed. Eng.*, vol. 50, no. 2, pp. 255–258, Feb. 2003.
- [10] W. R. Patterson, Y.-K. Song, C. W. Bull, A. P. Deangelis, C. Lay, J. L. McKay, A. V. Nurmikko, J. P. Donoghue, and B. W. Connors, “A microelectrode/microelectronic hybrid device for brain implantable neuroprosthetic applications,” *IEEE Trans. Biomed. Eng.*, vol. 51, no. 10, pp. 1845–1853, Oct. 2004.
- [11] D. A. Robinson, “The electrical properties of metal microelectrodes,” *Proc. IEEE*, vol. 56, no. 6, pp. 1065–1071, Jun. 1968.
- [12] P. E. K. Donaldson, “The essential role played by adhesion in the technology of neurological prostheses,” *Int. J. Adhesion Adhesives*, vol. 16, pp. 105–107, May 1996.
- [13] D. Edell. (2002, Dec.) Insulating biomaterials—First quarter progress report (NIH). InnerSea Technology, Bedford, MA. [Online] <http://www.ninds.nih.gov/qpr/electrode/N01-NS-9-2347QPR01.pdf>



Yoon-Kyu Song received the B.S. and M.S. degrees in electrical engineering from Seoul National University, Seoul, Korea, in 1992 and 1994, respectively, and the Ph.D. degree from Brown University, Providence, RI, in 1999.

He was a Research Scientist with Agilent Technologies, San Jose, CA, until rejoining Brown University as an Assistant Professor (Research) in 2003. His research interests include basic and applied semiconductor optoelectronics, such as vertical cavity lasers and nanostructured light emitters.



William R. Patterson (M'73) was born in Bronxville, NY, in 1941. He received the B.Sc. degree in physics and the M.Sc. degree in electrical engineering from Brown University, Providence, RI, in 1963 and 1966, respectively.

Since 1977, he has been with the Electrical Sciences Group, Division of Engineering, Brown University, where he is currently a Senior Lecturer and Senior Research Engineer. His research interests include low-power analog circuit design for biomedical applications, circuits and architectures for microphone array technology, and instrumentation for geological spectroscopy.

Mr. Patterson received the NASA Public Service Medal for contributions to the Viking Program in 1977.

Christopher W. Bull received the B.Sc. degree in mechanical engineering and the M.S. degree in electrical engineering from Brown University, Providence, RI, in 1979 and 1985, respectively.

He is currently a Senior Research Engineer and Lecturer at Brown University. His research interests include the neural-electronic interface, deformation of single crystals, and the strain rate dependence of material behavior.

Joseph Beals received the B.S. degree in electrical engineering from Brown University, Providence, RI, in 2004.

He worked as a Summer Research Intern for the Center for Manufacturing Innovation, Fraunhofer USA, Boston, MA, in 2001 and 2002. He is currently a Senior Research Assistant at Brown University, Providence. His research interests include the design and fabrication of novel semiconductor photo-voltaic devices.

Naejye Hwang received the B.S. degree from National Taiwan University, Taipei, Taiwan, R.O.C., and the M.S. degree from Brown University, both in electrical engineering. He is currently working toward the Ph.D. degree in the Department of Electrical Engineering, Princeton University, Princeton, NJ.

Andrew P. Deangelis was born in Providence, RI, in 1981. He received the B.Sc. degree in electrical engineering from Brown University, Providence, in 2003, where his research was focused on low-noise IC design and layout.

He is currently working as a Consultant for the Engineering Department, Brown University, and is a member of the Development Staff at Mathematical Systems Inc., Providence.

Christopher Lay received the B.Sc. degree in electrical engineering from Brown University, Providence, RI, in 2002.

He is currently with Texas Instruments, Attleboro, MA, where he is conducting research on circuits for automotive systems.

J. Lucas McKay received the B.Sc. and M.Sc. degrees in electrical engineering from Brown University, Providence, RI, in 2002 and 2003, respectively. He is currently working toward the Ph.D. degree at the Laboratory for Neuroengineering, Georgia Institute of Technology, Atlanta.

Arto V. Nurmikko (M'90–SM'97–F'99) was born in Finland. He received the B.S., M.S., and Ph.D. degrees in electrical engineering from the University of California, Berkeley.

He is currently the L. Herbert Ballou University Professor of Engineering and Physics at Brown University, Providence, RI. His research interests include basic and device science of wide bandgap semiconductors, studies of ultrafast processes in ferromagnetically ordered systems, and high-resolution imaging of neural circuits.

Prof. Nurmikko is a Fellow of the American Physical Society and the Optical Society of America.

Matthew R. Fellows received the B.A. degree in microbiology from the University of California, Santa Barbara, in 1994. He is currently working toward the Ph.D. degree in the Neuroscience Department, Brown University, Providence, RI, where his research involves the study of simultaneously recorded neural populations in primate motor cortex.

He then worked as a Research Assistant at the University of California, San Francisco, in a lab studying transgenic mouse models of cancer. While there, he developed an interest in systems neuroscience, which led him to the Laboratory of John Donoghue, Brown University.

John D. Simeral received the B.S. degree in electrical engineering from Stanford University, Stanford, CA, in 1985, the M.S. degree in electrical and computer engineering from the University of Texas at Austin in 1989, and the Ph.D. degree in neuroscience from Wake Forest University School of Medicine, Winston-Salem, NC, in 2003.

During his career as an Electrical Engineer, he served as a Project Manager of subsystem design and integration for one of AT&T's massively parallel terabyte computer systems, and held a 1995 Lectureship Position in the Department of Computer Science and Engineering, the University of California, San Diego. He is currently a Postdoctoral Fellow at Brown University, Providence, RI, where his research interests include the neural representation of movement, chronic multielectrode recording, BCI device integration, and algorithms for real-time decoding of neural signals in neuroprosthetic applications.

John P. Donoghue received the Ph.D. degree in neuroscience from Brown University, Providence, RI, in 1979.

He is currently the Henry Merritt Wriston Professor in and Chairman of the Department of Neuroscience, Brown University. He is a Co-Founder and Executive Director of Brown University's interdisciplinary Brain Science program, which includes physical, biological, and medical scientists, engineers, and mathematicians. He is also a Co-Founder and Chief Scientific Officer of Cyberkinetics, Inc., Foxborough, MA, a biotechnology startup that is developing neural prosthetics devices. His personal research program is aimed at understanding neural computations used to turn thought into movements and to produce brain machine interfaces that restore lost neurological functions.

Prof. Donoghue has received a Basil O'Connor Fellowship from the March of Dimes and a Javits Award from the National Institutes of Health.

Barry W. Connors received the Ph.D. degree in physiology and pharmacology from Duke University, Durham, NC, in 1979.

He is currently the L. Herbert Ballou University Professor of Neuroscience at Brown University, Providence, RI. His research interests include the cellular and synaptic physiology of the cerebral cortex and thalamus, the properties of electrical synapses, the behavior of small neural circuits, and the mechanisms of epileptic seizures.